

# Proton-Transfer Mediated Quenching of Pyrene/Indole Charge-Transfer States in Isooctane Solutions

Marcela S. Altamirano,<sup>†</sup> María del Valle Bohorquez,<sup>‡</sup> Carlos M. Previtali,<sup>†</sup> and Carlos A. Chesta<sup>†,\*</sup>

Departamento de Química, Universidad Nacional de Río Cuarto, 5800-Río Cuarto, Argentina

Received: August 6, 2007; In Final Form: October 6, 2007

The fluorescence quenching of pyrene (Py) by a series of *N*-methyl and *N*-H substituted indoles was studied in isooctane at 298 K. The fluorescence quenching rate constants were evaluated by mean of steady-state and time-resolved measurements. In all cases, the quenching process involves a charge-transfer (CT) mechanism. The  $I^0/I$  and  $\tau_0/\tau$  Stern–Volmer plots obtained for the *N*-H indoles show a very unusual upward deviation with increasing concentration of the quenchers. This behavior is attributed to the self-quenching of the CT intermediates by the free indoles in solution. The efficiency of quenching of the polyaromatic by the *N*-H indoles increases abruptly in the presence of small amount of added pyridine (or propanol). A detailed analysis of the experimental data obtained in the presence of pyridine provides unambiguous evidence that the self-quenching process involves proton transfer from the CT states to indoles.

## Introduction

The basic understanding of protein's structure and reactivity has triggered an important number of studies on the photophysics and photochemistry of tryptophan and related indolic compounds because they frequently act as the chief chromophores and redox centers of these macromolecules.

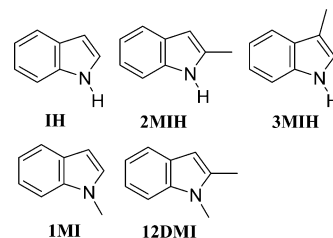
In this context, the quenching of the excited singlet state of pyrene (Py) by indolic compounds has been subject of many studies in both homogeneous<sup>1–3</sup> and microheterogeneous<sup>4–6</sup> media. It is well-established that Py fluorescence is quenched by indoles in polar and nonpolar solvents through a charge-transfer mechanism in which the indolic compounds behave as electron donors. It is also known that *N*-methyl indoles (MI) behave as quenchers quite differently compared to *N*-H indoles (IH). This difference has been explained in terms of the large acidity of the IH cation radical intermediates which are able to transfer a proton to the Py anion radical and produce a (reactive) pair of neutral radicals. The existence of the pyrenyl radical (PyH\*) and the radical ion radical of Py has been proved by laser flash photolysis experiments performed in polar solvents.<sup>3</sup> Similar results were found when anthracene<sup>7,8</sup> and a cyanoanthracene<sup>9</sup> where used as electron acceptor.

We report here a study on the quenching of Py singlet excited state by the indoles (Chart 1) in isooctane. It was found that the quenching of the aromatic by the *N*-H indoles represents a very interesting example in chemical kinetics. For this quenchers, the Stern–Volmer (SV) plots constructed from either steady-state intensities or time-resolved measurements show an unusual upward curvature. Evidence is provided to demonstrate that the photoreaction involves proton transfer from the charge-transfer (CT) intermediate to the free indoles in solution.

## Experimental Section

Pyrene from Merck was purified by recrystallization from methanol. Indole (IH) (Aldrich) was used without further

## CHART 1



purification. 1-Methylindole (1MI), 2-methylindole (2MIH), 3-methylindole (3MIH), and 1,2-dimethylindole (12DMI) were from Sigma, and they were purified by vacuum distillation, recrystallization and sublimation, respectively. Pyridine (Merck) and isooctane (Sintorgan, HPLC grade) were used without further purification.

Absorption spectra were recorded using a HP 8453 UV–visible spectrophotometer.

Stationary fluorescence quenching experiments were carried out using a Spex Fluoromax spectrofluorometer. Typically,  $5 \times 10^{-6}$  M solutions of Py were employed for fluorescence studies. Samples were excited at 338 nm. All measurements were performed in deoxygenated solutions at  $298 \pm 1$  K.

Lifetime measurements were performed by using the time-correlated single photon-counting technique (TCSPC) with an Edinburgh Instruments OB900 apparatus. Criteria used to judge the goodness of the fits were  $\chi^2$  and the weighted residuals ( $R_i$ ). The decays curves were rejected when visual inspection of  $R_i$  vs channel number showed nonrandom behavior. For  $\chi^2$  the maximum allowed was 1.25.

Continuous photolysis experiments were performed with a monochromatic illumination system (Photon Technology International) equipped with a 75 W xenon arc lamp. Samples were excited at 338 nm. Aberchrome 540 was used as actinometer according to the experimental procedure described in the literature.<sup>5</sup>

Laser flash photolysis experiments were carried out using a nitrogen laser (Laseroptics, 5 ns fwhm, 5 mJ pulses). The laser flash photolysis setup was described previously.<sup>10</sup>

\* Corresponding author. E-mail cchesta@exa.unrc.edu.ar.

<sup>†</sup> Departamento de Química, UNRC, Río Cuarto, Argentina.

<sup>‡</sup> College of Arts and Sciences, Drake University, Des Moines, Iowa.

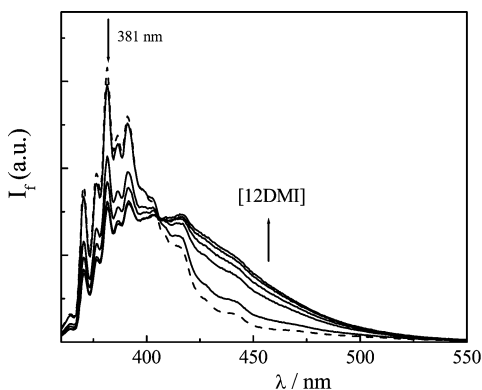


**Figure 1.** Fluorescence emission spectrum of Py in isoctane at 298 K in the absence (---) and in the presence of 12DMI 0.009, 0.023, 0.033, 0.043, and 0.05 M.

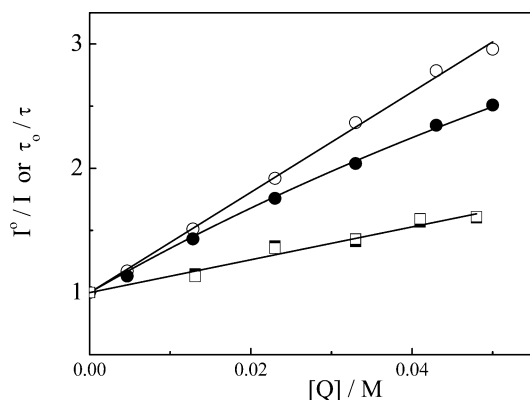


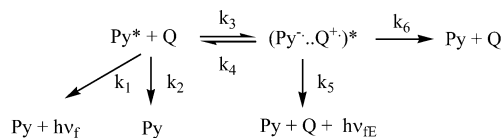
**Figure 2.** Quenching of Py by 12DMI (○, ●) and 1MI (□, ■) in isoctane at 298 K. The open symbols represent the results from the steady-state experiments. The solid lines correspond to the fitting of the experimental data to eqs 1 and 4, respectively. See the text for details.

## Results and Discussion

**Quenching of Pyrene by *N*-Methyl Indoles.** A comprehensive study on the quenching of the singlet excited state of Py and other Py derivatives by 12DMI in polar and nonpolar solvents was previously reported by Palmans et al.<sup>1</sup> In isoctane the quenching is accompanied by the appearance of a new red-shifted structureless emission around 425 nm as shown in Figure 1. The fluorescence decay curves analyzed either at 381 nm (Py emission) or at 485 nm (exciplex emission) yielded single-exponential decays with the same decay parameters. These results are clear evidence of reversible exciplex formation.<sup>11,12</sup> Typical Stern–Volmer (SV) plots constructed from the dependence of the polyaromatic steady-state emission intensities ( $I^0/I$ ) and lifetimes ( $\tau_0/\tau$ ) on [12DMI] are shown in Figure 2. As it can be concluded, the  $I^0/I$  and  $\tau_0/\tau$  SV plots are not equivalent. Furthermore, although the  $I^0/I$  is linear ( $K_{SV} = 40.3 \text{ M}^{-1}$ ), the  $\tau_0/\tau$  plot shows a slight downward curvature.

The quenching of Py emission by 1MI in isoctane does not show evidence of exciplex formation. The SV plot constructed from the changes of the Py emission (381 nm) is linear. The experimental  $K_{SV}$  obtained from the experimental data in Figure 2 is  $\sim 13 \text{ M}^{-1}$ . The Py emission decays always monoexponentially at all the concentrations of the quencher studied. In contrast to that observed in the case of the Py/12DMI system, the SV plot constructed from the experimental  $\tau$  is also linear and, within experimental uncertainties, indistinguishable from the  $I^0/I$  plot.

## SCHEME 1



Results above can be explained by the mechanism in Scheme 1 where  $\text{Py}^*$  represents the singlet excited state of the fluorophore, Q is the indolic quencher, and  $(\text{Py}^{\cdot-} \cdots \text{Q}^{\cdot+})^*$  stands for the CT state. Within the framework of Scheme 1, the dependence of the stationary Py emission intensity ( $I$ ) on [Q] is given by

$$\frac{I^0}{I} = 1 + \frac{k_3\tau_0}{(1 + k_4\tau_e)} [\text{Q}] = 1 + k_q\tau_0[\text{Q}] \quad (1)$$

$$K_{SV}/\tau_0 = k_q = \frac{k_3}{(1 + k_4\tau_e)}$$

where  $\tau_0 = 1/(k_1 + k_2)$  represents the lifetime of the fluorophore and  $\tau_e = 1/(k_5 + k_6)$  that of the CT intermediate. The expression for the time dependent concentration of  $[\text{Py}^*(t)]$  is given by<sup>11,12</sup>

$$[\text{Py}^*(t)] = a_1 \exp(-\lambda_1 t) + a_2 \exp(-\lambda_2 t) \quad (2)$$

where

$$\lambda_{1,2} = \frac{1}{2} \{ (X + Y) \mp [(X - Y)^2 + 4k_3k_4[\text{Q}]]^{1/2} \} \quad (3)$$

$$X = \frac{1}{\tau_0} + k_3[\text{Q}] \quad Y = \frac{1}{\tau_e} + k_4 \quad \frac{a_2}{a_1} = \frac{(X - \lambda_1)}{(\lambda_2 - X)}$$

According to eq 2, the fluorophore emission should always follow a biexponential decay.<sup>13</sup> In practice, the possibility of solving the biexponential decay, i.e., the possibility of obtaining genuine values for  $\lambda_1$  and  $\lambda_2$ , depends on the resolution of the instrumental used.<sup>14</sup> There are two particular kinetic cases that stress the instrumental resolution to the limit: (a) irreversible exciplex formation; which is associated with the kinetic limit condition  $k_4 \ll 1/\tau_e$ , and (b) rapid excited-state equilibrium, which is observed when the system studied satisfies (simultaneously) the conditions  $k_3 \gg 1/\tau_0$  and  $k_4 \gg 1/\tau_e$ . In the first case, fast exciplex deactivation makes  $a_2/a_1 \gg 1$  and only  $\lambda_2$  can be determined. From the value of  $\lambda_2$  ( $\cong 1/\tau_0 + k_3[\text{Q}]$ ) the well-known Stern–Volmer expression can be derived. In the second case, either  $1/\lambda_2$  or  $a_2/a_1$  (or both) are likely to vanish and the apparent monoexponential decay is attributed to  $\lambda_1$ . From the dependency of  $\lambda_1$  on [Q], the following equation can be derived:<sup>11,12,15</sup>

$$\frac{\tau_0}{\tau} \cong \frac{1 + \left(\frac{k_3\tau_0}{k_4\tau_e}\right)[\text{Q}]}{\left[1 + \left(\frac{k_3}{k_4}\right)[\text{Q}]\right]} \quad (4)$$

As a result, the plots obtained from steady-state  $I^0/I$  (eq 1) and time-resolved  $\tau_0/\tau$  (eq 4) measurements do not correspond. In addition, the  $\tau_0/\tau$  plot must show a downward deviation which magnitude depends on the equilibrium constant  $K_{34}(=k_3/k_4)$ .

Hence, the negative deviation from linearity in the  $\tau_0/\tau$  plot shown in Figure 2 suggests that the quenching mechanism involves a rapid exciplex equilibrium. From the fitting of the

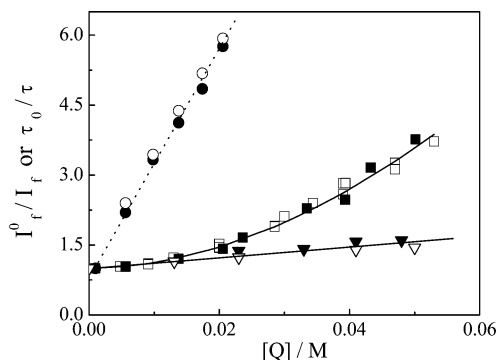


**Figure 3.** Quenching of Py by IH in isooctane at 298 K.  $I^0/I_f$  plots in neat solvent (■) and in the presence of pyridine 0.1 M (●).  $\tau_0/\tau$  plots in the absence (□) and in the presence of pyridine 0.1 M (○). See the text for details. Quenching of Py by 1MI,  $I^0/I_f$  plots in neat isooctane (▼) and in the presence of pyridine 0.1 M (▽).

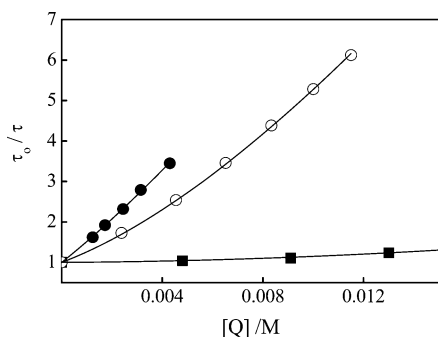


**Figure 4.** Quenching of Py by 3MI (●), 2MI (○), and IH (■) (initial points from Figure 3) in isooctane at 298 K. The solid line represents the fitting of the  $\tau_0/\tau$  data to eq 10 and the parameters are given in Tables 1 and 2. See the text for details.

experimental  $\tau_0/\tau$  to eq 4 and  $\tau_0 = 400 \pm 10$  ns we obtained  $K_{34}/\tau_e = (1.1 \pm 0.1) \times 10^8 \text{ M}^{-1} \text{ s}^{-1}$  and  $K_{34} = 5 \pm 2 \text{ M}^{-1}$  and, therefore,  $\tau_e = 47 \pm 7$  ns. The value of  $k_q = (1.01 \pm 0.05) \times 10^8 \text{ M}^{-1} \text{ s}^{-1}$ , obtained from the fitting of the  $I^0/I_f$  plot, is practically the same as  $K_{34}/\tau_e$ , suggesting that  $k_4\tau_e > 10$  and, therefore,  $k_3 > 1 \times 10^9 \text{ M}^{-1} \text{ s}^{-1}$ .

On the other hand, the results obtained for the system Py/1MI do not allow distinguishing between the irreversible and the reversible exciplex mechanism. However, based in simple thermodynamic considerations (*vide infra*), it is possible to conclude that the agreement observed between the  $I^0/I_f$  and  $\tau_0/\tau$  plots is the consequence of a small value of  $K_{34}$ .

**Quenching of Pyrene by H–N Indoles (IH).** The fluorescence quenching of Py by H–N indoles in isooctane presents some particular features common to the three indoles investigated.

The quenching process takes place without distortions of the emission spectrum of Py, and therefore, the formation of emissive CT intermediates (exciplexes) can be disregarded. The SV plots obtained from steady-state fluorescence experiments ( $I^0/I_f$ ) show an unambiguous upward curvature. Py emission decay curves followed single monoexponential decays at all concentrations of the quenchers studied. Interestingly, the  $\tau_0/\tau$  plots also show an upward curvature and differ slightly from the  $I^0/I_f$  plots. In Figure 3, the  $I^0/I_f$  and  $\tau_0/\tau$  plots for the quenching of Py by IH in isooctane are shown. In Figure 4 the corresponding  $\tau_0/\tau$  plots for 2MIH, 3MIH, and IH are compared. As can be concluded from Figure 4, the quenching by 2MIH and 3MIH is much more efficient than the quenching by IH. Similar results were found when the quenching experiments were carried out in cyclohexane or n-heptane.

**TABLE 1: Kinetic Parameter Obtained for the Quenching of Py by Indolic Compounds in Chart 1 in Isooctane at 298 K**

quencher	$E_{ox}^a$	$pK_a^b$	$k_3/(10^9 \text{ M s})$	$K_{34}$	$\tau_e/\text{ns}$	$k_q/(10^9 \text{ M s})$
IH	1.24	4.9	$1.1 \pm 0.1$	$2 \pm 1$	$80 \pm 20$	$1.1 \pm 0.6$
1MI	1.23			$< 2$	0	0
12DMI	1.12		$> 1$	$5 \pm 2$	$47 \pm 7$	0
2MIH	1.10	5.7	$5.0 \pm 0.4$	$25 \pm 5$	$39 \pm 4$	$2.4 \pm 0.1$
3MIH	1.07	5.0	$7.5 \pm 0.9$	$50 \pm 40$	$40 \pm 4$	$1.9 \pm 0.2$

<sup>a</sup> The oxidation potentials were taken from ref 21, with exception of the value reported for 12DMI that was obtained from ref 8. <sup>b</sup> Reported errors correspond to one standard deviation.

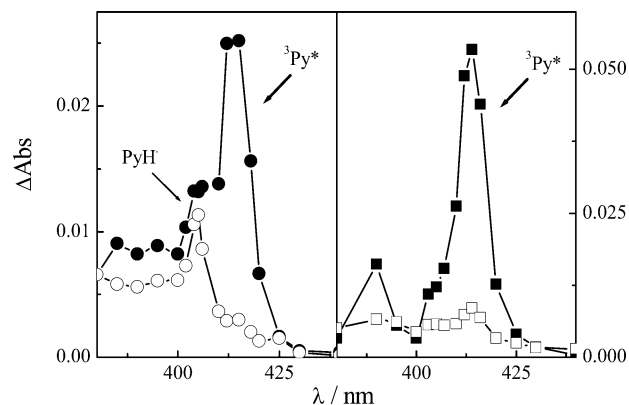
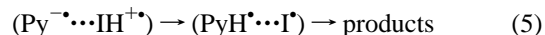


**Figure 5.** Left panel: transient absorption spectra of Py/IH (0.1 M) in isooctane 1.4  $\mu\text{s}$  (●) and 40.0  $\mu\text{s}$  (○) after the laser pulse. Right panel: transient spectra of Py/1MI (0.1 M) in isooctane 1.4  $\mu\text{s}$  (■) and 40.0  $\mu\text{s}$  (□) after the laser pulse.

Another common feature of the Py/N–H indoles systems is their photoreactivity. When Py in isooctane is irradiated continuously at 338 nm in the presence of the N–H indoles, bleaching of the Py absorption and the appearance of a new broad red-shifted absorption band are observed in all cases. The existence of isobestic points suggests clean photochemical reactions. This photoreaction is exclusive of the N–H indoles derivatives and its quantum efficiency depends on the structure of the indole quencher and on the polarity of the medium. It has been proposed that “in cage” proton transfer occurring in the exciplex intermediate followed by combination of the radicals is the source of the observed absorption bleaching. The photoreaction can be schematized as follows:



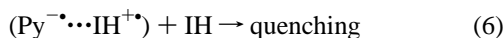
Proton transfer from the indole cation radicals ( $\text{IH}^{\cdot+}$ ) to the Py radical anion is favored by the increased acidity of the indoles in their oxidized forms. The  $pK_a$  of the  $\text{IH}^{\cdot+}$  are listed in Table 1. In polar solvents such as acetonitrile, methanol and acetone, the presence of the  $\text{Py}^{\cdot-}$ ,  $\text{PyH}^{\cdot}$ , and  $\text{IH}^{\cdot+}$  was confirmed by laser flash photolysis experiments.<sup>3</sup> The transient absorption spectra of Py/IH (0.1 M) in isooctane are shown in Figure 5 (left panel). The spectrum obtained 1.4  $\mu\text{s}$  after laser pulse shows a strong absorption around 415 nm, an absorption that is assigned to the Py triplet excited state. The triplet of the Py fluorophore is formed directly from the (singlet) CT intermediate *via* fast intersystem crossing.<sup>3</sup> The transient spectrum taken 40  $\mu\text{s}$  after the laser pulse shows only the absorption due to the neutral radical  $\text{PyH}^{\cdot}$ .<sup>16</sup> The lack of absorption signals that could be assigned to  $\text{Py}^{\cdot-}$  and  $\text{IH}^{\cdot+}$  indicates that CT recombination occurs in a shorter time scale ( $< 1 \mu\text{s}$ ). In contrast, the transient spectra for Py/1MI (0.1 M) system in isooctane (Figure 5, right panel) show the formation of  $^3\text{Py}^*$  as the only important species present in the same time window.

Hence, taking into account the laser flash photolysis experiments in Figure 5 and the large quantum efficiencies observed for the photoreactions of the IH in isoctane (eq 5), it seems reasonable to suppose that the same type of intermediates are been produced in polar and nonpolar solvents. However, it seems also clear that the upward curvature of the SV plots observed for N–H indoles cannot be explained in terms of Scheme 1.

Several mechanisms may explain this unusual behavior.

A mechanism that deserves consideration is (H-bond) ground-state association of the H–N indoles, i.e.,  $2 \text{ IH} = (\text{IH})_2$ , combined with an increased capacity of the dimer form for quenching the emission of the polyaromatic. However, no evidence for association of HI were found in nonpolar solvents, as could be possible to detect by  $^1\text{H}$  NMR, IR, and UV-absorption spectroscopy.<sup>17</sup> Hence, this mechanism can be disregarded. Ground-state donor (IH)/acceptor (Py) interactions producing a combination of dynamic/static quenching processes can be also ruled out because the absorption spectrum of the polyaromatic does not change in the presence of the indolic quenchers. In addition, when this type of mechanism is operative, upward curved  $I^0/I$ , but lineal  $\tau_0/\tau$  SV plots, are observed.

An alternative possibility involves quenching of the CT intermediate by the free indole in solution as represented in eq 6.



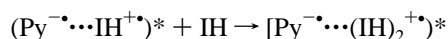
Taking into account this new deactivation process of the CT intermediate in Scheme 1, the dependence of the Py stationary emission on the concentration of the quencher is given by

$$\frac{I^0}{I} = 1 + k_3\tau_0[\text{Q}] \left[ \frac{(1 + k_7\tau_e[\text{Q}])}{(1 + k_4\tau_e + k_7\tau_e[\text{Q}])} \right] \quad (7)$$

which correctly predicts the nonlinear dependence of the  $I^0/I$  plot. Similarly, if it is assumed that the systems studied satisfy the conditions of the rapid equilibrium limit, i.e.,  $k_3 \gg 1/\tau_0$  and  $k_4 \gg 1/\tau_e + k_7[\text{Q}]$ , the corresponding  $\tau_0/\tau$  plots can be interpreted according to<sup>18</sup>

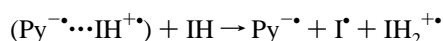
$$\frac{\tau_0}{\tau} \cong \frac{1 + \left(\frac{k_3\tau_0}{k_4\tau_e}\right)[\text{Q}](1 + k_7\tau_e[\text{Q}])}{\left[1 + \left(\frac{k_3}{k_4}\right)[\text{Q}]\right]} \quad (8)$$

Again, at least two different mechanisms can account for the CT quenching process in eq 7. A plausible explanation involves the formation of a short-lived ternary CT state<sup>19</sup> (or exterples) *via* charge-transfer interactions between the polar intermediate and the free indole:



However, this mechanism can be ruled out because it should be also possible for 12MI and MI, which show “normal” quenching behaviors.

A second possibility involves  $\text{H}^+$  transfer from the CT states to the free indole in solution:



As commented above, protons transfer from  $\text{IH}^{\cdot+}$  to  $\text{Py}^{\cdot-}$  is responsible for the bleaching of the polyaromatic absorption in

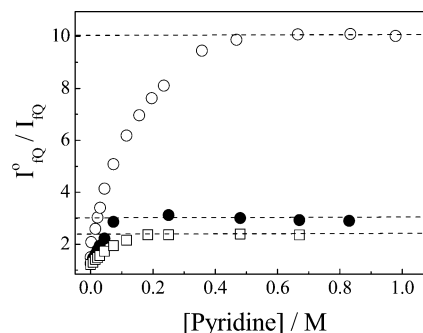
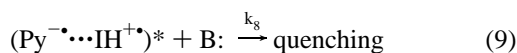


**Figure 6.** Effect of added pyridine on the quenching efficiency at constant concentrations of IH  $2 \times 10^{-2}$  M (○), 2MIH  $1 \times 10^{-3}$  M (●), and 3MIH  $5 \times 10^{-4}$  M (□). All experiments were carried out in isoctane at 298 K.

the continuous photolysis experiments. Although the  $pK_b$  values for indole and structurally related compounds have not been reported (which is in line with their low expected basicity), the IHs should be basic enough to compete with the anion radical of Py. Evidence for this mechanism was found by reinvestigating the systems in the presence of 1-propanol and pyridine (B:), two bases that would be able to compete with the free IH in a hypothetical  $\text{H}^+$ -transfer quenching process of the CT intermediate. These bases were selected because they do not absorb at the excitation wavelength and they do not affect the lifetime of the Py fluorophore at  $[\text{B}:] < 1$  M. The  $I^0/I$  and  $\tau_0/\tau$  SV plots obtained for the Py/IH system in the absence and presence of 0.1 M pyridine are compared in Figure 3. The effect of the base is remarkable; the apparent efficiency of the quenching process increases abruptly whereas the quadratic-like dependence on  $[\text{IH}]$  disappears. Less significant effects were observed when 1-propanol (0.1 M) was used as base. Importantly, similar enhancements of the quenching efficiency were also found when the Py/2MIH and Py/3MIH systems were investigated in the presence of bases, but no effects were observed in the case of Py/12MI and Py/1MI. The  $I^0/I$  plots for the system Py/1MI in neat isoctane and in the presence of pyridine are shown in Figure 3.

Hence, assuming that the presence of the base adds a new (competing) deactivation process to the CT intermediate in Scheme 1:



the following expression can be derived:

$$\frac{I_Q^0}{I_Q} = 1 + k_3\tau_0[\text{Q}] \left[ \frac{1 + k_7\tau_e[\text{Q}] + k_8\tau_e[\text{B} :]}{1 + k_4\tau_e + k_7\tau_e[\text{Q}] + k_8\tau_e[\text{B} :]} \right] \quad (10)$$

where the subscript Q indicates that the fluorophore emission intensities ( $I_Q$ ) are measured at a constant concentrations of Q, while  $[\text{B} :]$  is varied. In Figure 6, the experimental  $I_Q^0/I_Q$  are plotted as a function of the concentration of pyridine for the Py/N–H indole systems. According to eq 10, the  $I_Q^0/I_Q$  ratio must increase with increasing  $[\text{B} :]$  until a plateau is reached at sufficiently large concentrations of the base. The plateau is achieved when  $k_8\tau_e[\text{B} :] \gg (1 + k_4\tau_e + k_7\tau_e[\text{Q}])$ , and therefore, the plateau value of the  $I_Q^0/I_Q$  plots, i.e.,  $\cong 1 + k_3\tau_0[\text{Q}]$ , can be used for the estimation of  $k_3$ . The  $k_3$  values are collected in Table 1.

Additional information on the kinetics of the quenching processes can be obtained by analyzing the  $I^0/I$  and  $\tau_0/\tau$  SV plots. For instance, eq 7 can be rearranged to give

$$G = \frac{I^0/I - 1}{(k_3\tau_0[Q] + 1) - I^0/I} = \frac{1}{k_4\tau_e} + \frac{k_7}{k_4}[Q] \quad (11)$$

Assuming that the values of  $k_3\tau_0$  are known (Table 1), approximated values for  $k_4\tau_e$  and  $k_7/k_4$  can be estimated from the intercepts and slopes of the  $G$  vs  $[Q]$  plots. Figure 7, shows the plots for the Py/IHs. The values of  $k_4\tau_e$  and  $k_7/k_4$  are collected in Table 2.<sup>20</sup>

To calculate the values of  $K_{34}$ ,  $k_7$ , and  $\tau_e$ , we fitted the  $\tau_0/\tau$  plots (Figure 3 and 4) to eq 8, taking  $k_7$  and  $\tau_e$  as adjustable parameters and assuming that the values of  $k_3$  (Table 1) and  $k_4$  ( $=k_7/\text{slope}$ , Table 2) are known. Unfortunately, this fitting procedure is quite sensitive to the experimental uncertainties and to the assumed values of  $k_3$  and  $k_4$ . Therefore, the values of  $K_{34}$ ,  $k_7$ , and  $\tau_e$  listed in Table 1 must be considered as rough estimates.

An analysis of the data in Table 1 shows that  $k_3$  increases with decreasing oxidation potential of the indole quenchers. The  $K_{34}$  show a similar dependence on  $E_{ox}$ . These results are in agreement with the expected electron-transfer nature of the initial step of the photoreaction. In Table 2 we also report the values of  $K_{SV}$  (eq 1) calculated using the data in Table 1. This quantity represents the SV constant measured at infinite dilution of the quenchers (the initial slope of the  $I^0/I$  plots for the case of the N–H quenchers). The  $K_{SV}$  values for the quenching by IH and IMI agree satisfactorily, suggesting that the magnitude of the rate constants controlling the quenching processes are similar, as could be anticipated from their similar  $E_{ox}$ . Finally, the  $k_7$  are consistently  $\sim 10^9 \text{ M}^{-1} \text{ s}^{-1}$ , one order of magnitude smaller than the diffusion limit in isoctane. The value of  $k_7$  should depend on both, the acidic capability of the  $\text{IH}^{+\bullet}$  and the basicity of indole quenchers.

In summary, the quenching of Py by *N*-methyl and N–H indoles share a common mechanism that involves initially the formation a reversible CT state. In the case of the N–H quenchers, the CT intermediate can be intercepted by the free indole in solution. This effect leads to a shift of the dynamic equilibrium and to an apparent increased quenching capability. Although the self-quenching of exciplexes is a very well documented phenomenon, to our knowledge, the results reported

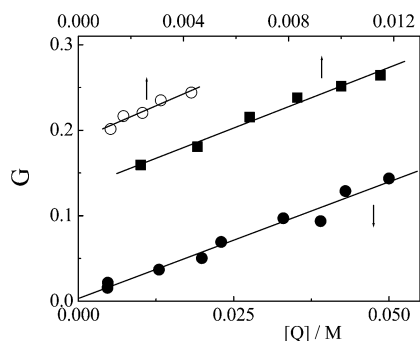


**Figure 7.** Plots of  $G$  vs  $[Q]$  according to eq 13: IH (●), bottom scale; 2MIH (■) and 3MIH (○), top scale. All experiments were carried out in isoctane at 298 K.

**TABLE 2: Kinetic Parameters Obtained from the Analysis of the Plots in Figure 4 (Details in Text)**

quencher	$(k_7/k_4)/\text{M}^{-1}$	$k_4\tau_e$	$K_{SV}/\text{M}^{-1}$
IH	$2.7 \pm 0.2$	$300 \pm 400$	$11 \pm 4$
IMI	0		$13.3 \pm 0.5$
12DMI	0		$40.3 \pm 0.6$
2MIH	$11.9 \pm 0.7$	$7.6 \pm 0.3$	$280 \pm 60$
3MIH	$13 \pm 2$	$5.3 \pm 0.3$	$500 \pm 100$

here represent the first case of proton-transfer mediated quenching of a CT state described in literature.

**Acknowledgment.** We thank to the Consejo Nacional de Investigaciones Científicas y Técnicas (CONICET-Argentina), Agencia Nacional de Promoción Científica (FONCYT-Argentina), and Secretaría de Ciencia y Técnica de la Universidad Nacional de Río Cuarto for the financial support.

## References and Notes

- (1) (a) Palmans, J. P.; Van der Auweraer, M.; Swinnen, A. M.; De Schriver, F. C. *J. Am. Chem. Soc.* **1984**, *106*, 7721. (b) Helsen, N.; Viaene, M.; Van der A Auweraer M.; De Schriver, F. C. *J. Phys. Chem.* **1994**, *98*, 1532. (c) Swinnen, A. M.; Ruttens, M.; van del Auweraer, M.; Schryver, F. C. *Chem. Phys. Letts* **1985**, *116*, 217.
- (2) Montejano, H. A.; Cosa, J. J.; Garrera, H. A.; Previtali, C. M. *J. Photochem. Photobiol. A: Chem.* **1995**, *86*, 115.
- (3) (a) Borsarelli, C. D.; Montejano, H. A.; Cosa, J. J.; Previtali, C. M. *J. Photochem. Photobiol. A: Chem.* **1995**, *91*, 13. (b) Montejano, H. A.; Cosa, J. J.; Garrera, H. A.; Previtali, C. M. *J. Photochem. Photobiol. A: Chem* **1995**, *86*, 115. (c) Altamirano, M. S.; Borsarelli, C. D.; Cosa, J. J.; Previtali, C. M. *J. Colloid Interface Sci.* **1998**, *205*, 390.
- (4) Miyoshi, N.; Tomita, G. *Photochem. Photobiol.* **1979**, *29*, 527.
- (5) Encinas, M. V.; Lissi, E. A. *Photochem. Photobiol.* **1985**, *42*, 491.
- (6) Encinas, M. V.; Lissi, E. A. *Photochem. Photobiol.* **1986**, *44*, 579.
- (7) Encinas, M. V.; Previtali, C. M.; Bertolotti, S. G. *J. Chem. Soc., Faraday Trans.* **1996**, *92*, 17.
- (8) (a) Novaira, A. I.; Borsarelli, C. D.; Cosa, J. J.; Previtali, C. M. *J. Photochem. Photobiol. A: Chem.* **1998**, *115*, 43. (b) Novaira, A. I.; Avila, V.; Montich, G. G.; Previtali, C. M. *J. Photochem. Photobiol. B: Biol.* **2001**, *60*, 25.
- (9) Pal, S. K.; Bhattacharya, T.; Misra, T.; Saini, R. D.; Ganguly, T. *J. Phys. Chem. A.* **2003**, *107*, 10243.
- (10) Avila, V.; Cosa, J. J.; Previtali, C. M. *An. Asoc. Quím. Argent.* **1990**, *78*, 279.
- (11) Ware, W. R.; Watt, D.; Holmes, J. D. *J. Am. Chem. Soc.* **1974**, *96*, 7853.
- (12) Birks, J. B.; Dynson, D. J.; Munro, I. H. *Proc. R. Soc. London, Ser. A* **1963**, *275*, 575.
- (13) Similarly, exciplex emission also follows a biexponential decay according to  $[(\text{Py}^{\bullet-}\cdots\text{Q}^{\bullet+})(t)] = a_3 \exp(-\lambda_1 t) - a_4 \exp(-\lambda_2 t)$ . Further details are given in refs 11 and 12.
- (14) For the instrumental used in this study the resolution can be set as  $1/\lambda_1, 1/\lambda_2 > 0.5 \text{ ns}$  and  $20 > a_1/a_2 > 1$ .
- (15) (a) Birks, J. B. *Photophysics of Aromatic Molecules*; Wiley: New York, 1970; Chapter 7. (b) Kuzmin, M. G. *Pure Appl. Chem.* **1993**, *65*, 1653. (c) Kiyota, T.; Yamaji, M.; Shizuka, H. *J. Phys. Chem.* **1996**, *100*, 672.
- (16) Okada, T.; Karaki, I.; Mataga, N. *J. Am. Chem. Soc.* **1982**, *104*, 7191.
- (17) Horrocks, D. H. *J. Chem. Phys.* **1969**, *50*, 4151 and reference therein.
- (18) *A priori*, it is impossible to guarantee that the approximation  $k_4 \gg 1/\tau_e + k_7[Q]$  holds valid at all the concentrations of quencher. In any case, the  $\tau_0/\tau$  plots can be fitted directly to the expression of  $\lambda_1$  (eq 3), which does not involve any approximation, according to
 
$$\frac{\tau_0}{\tau} = \frac{\lambda_1}{\lambda_{10}} = \tau_0 \{ (X + Y) - [(X - Y)^2 + 4k_3k_4[Q]]^{1/2} \}$$

$$X = 1/\tau_e + k_3[Q] \quad Y = 1/\tau_e + k_4 + k_7[Q]$$
- (19) (a) Beens, H.; Weller, A. *Chem. Phys. Lett.* **1968**, *2*, 140. (b) Taylor, G. N.; Chandross, E. A.; Schiebel, H. G. *J. Am. Chem. Soc.* **1974**, *96*, 2730. (c) Mimura, T.; Itoh, M. *Bull. Chem. Soc. Jpn.* **1977**, *50*, 1739. (d) Chesta, A.; Avila, V.; Soltermann, A. T.; Crystall, B.; Phillips, D.; Cosa, J. J. *J. Chem. Soc., Faraday Trans.* **1996**, *92*, 3327.
- (20) The values of  $k_4\tau_e$  and  $k_7/k_4$  could be also obtained by fitting the (curved)  $I^0/I$  plots. However, the plots according eq 13 provide an unambiguous visualization the self-quenching processes.
- (21) Merenyi, G.; Lind, J.; Shen, X. *J. Phys. Chem.* **1988**, *92*, 134.